

A PRECISE INDUCTION MOTOR SPEED ESTIMATOR, BASED ON A FIXED CARRIER FREQUENCY SIGNAL

Juan W. Dixon and José N. Rivarola
 Dept. of Electrical Engineering
 Universidad Católica de Chile
 Casilla 306, Correo 22
 Santiago, Chile
 FAX +56-2-552-2563

Abstract.— A speed estimation method, based on the introduction of a constant frequency carrier signal, is presented. This frequency carrier signal produces a constant speed rotating field from which the speed information in a wide range is obtained. The speed is estimated through the detection of irregularities in the rotor. These irregularities generate frequency pulsations proportional to the rotor speed, which are independent of the parameters of the machine. Because these signals are extremely low, special electronic circuits, implemented with analog multipliers and filters, have been designed, and they are able to measure very low speed values. Computer simulations and some experiments have been carried out, and they have shown that it is possible to measure speeds as low as 20 rpm.

I INTRODUCTION

The recent advances in power electronics have permitted the implementation of sophisticated methods of control for induction machines, such as vector control [1-2], slip frequency control [3], flux oriented control [2-4] and others. All these drives require a precise estimation of rotor speed. Traditionally, mechanical tachometers have been used, but they have the disadvantage of having mechanical problems and maintenance requirements. Recently, numerous attempts to estimate the speed machine without tachometer are being done, most of them based on the knowledge of the parameters of the machine [5]. With this method, the flux, torque or speed can be evaluated to control the motor. However, the parameters of the machine are not constant because they depend strongly on machine temperature and saturation of the magnetic circuit. In recent years, a novel method, based on small rotor irregularities has been reported [6-8]. This method is independent of the parameters of the machine but is difficult to operate with variable frequency systems. Besides, it cannot measure low speeds with precision, because it is not possible to isolate and filter the side bands from the low frequencies of the inverter. This paper presents a different method, based on the introduction of a fixed high frequency carrier voltage (300 to 400 Hz), which is added to the normal frequency of the inverter, to feed the machine terminals. The high speed rotating field produced by this carrier allows to detect, through specially designed circuits, an important number of side-band frequency components of the carrier, produced by the irregularities in the rotor.

II SPEED ESTIMATION

As it was already mentioned, the speed estimation method is realized adding to the output frequency inverter, a fixed frequency carrier signal. To avoid problems with the isolation of the speed signals, the rotating field of this carrier should not interfere with the inverter frequency. If the inverter works in the region 0-100 Hz, the carrier signal has to be bigger than 100 Hz. 400 Hz has been chosen for this carrier signal, which is far from the main frequency and permits to generate more than one left-side-band frequency. In this form, the carrier frequency and their side-bands generated, can be easily isolated from the inverter frequency operation. The side-band frequencies are produced by rotor slots and eccentricities and move when the speed machine changes. According with reference [6], they can be evaluated through the following equations:

$$f_{sb1} = f_c \left[(n \cdot R \pm n_e) \cdot \left(\frac{1-s}{p} \right) \pm n_{vs} \right] \quad (1)$$

$$f_{sb2} = f_c \cdot \left[(n \cdot R \pm n_e \pm n_r \cdot p) \cdot \left(\frac{1-s}{p} \right) \pm n_{vr} \right] \quad (2)$$

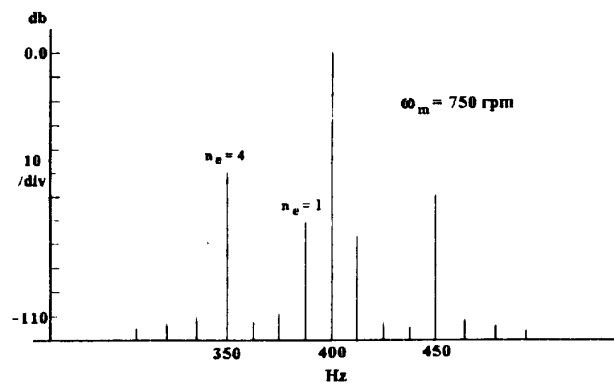


Fig. 1. Carrier frequency spectrum

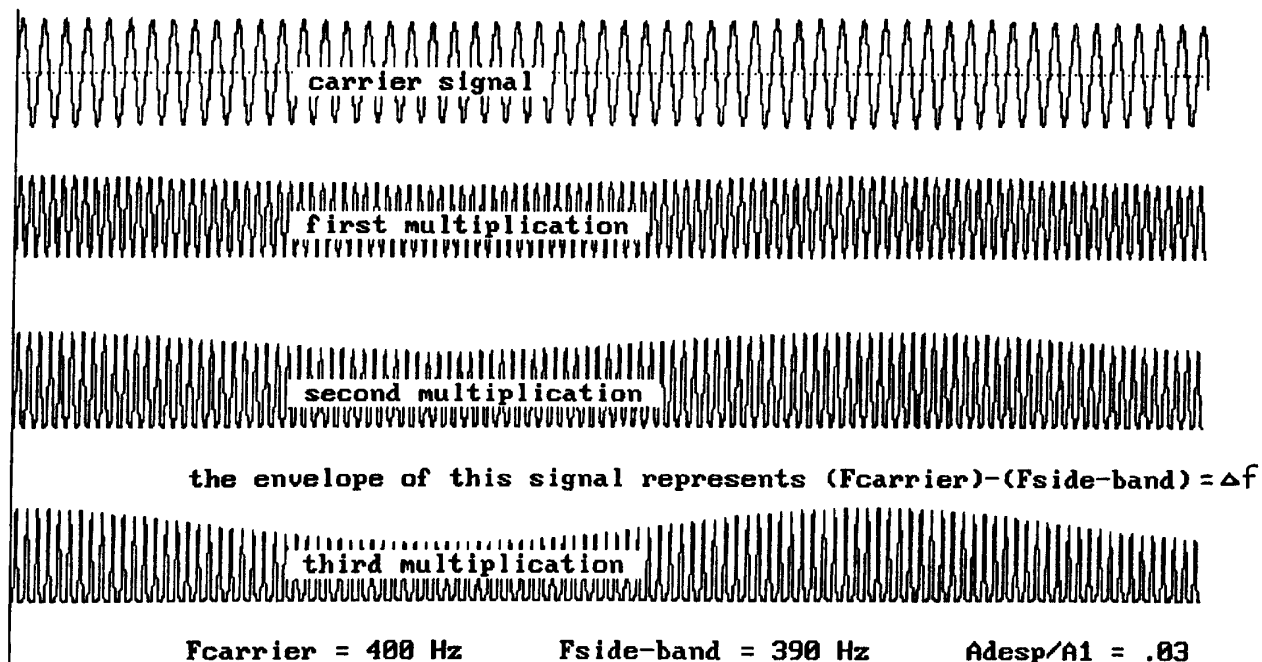


Fig. 2. Detection of Δf using analog multipliers.

where:

- $i = 1$ (main frequency); 2 (carrier frequency)
- f_{sb} : side-band frequency generated
- R : number of rotor slots
- n : any integer = 0, 1, 2, 3,...
- n_{st} : order number of stator mmf time harmonic = 1, 2, 3,...
- n_{r} : order number of rotor mmf time harmonic = 1, 2, 3,...
- n_s : rotor space harmonic number = 1, 2, 3,...
- n_d : dynamic excentricity number = 1, 2, 3,...
- f_1 : fundamental frequency
- s_1 : slip relative to f_1
- p : number of pairs of poles

These side-band frequencies can be displayed in the frequency domain, to get the spectrum of Fig.1, for a 400 Hz frequency carrier. The relative magnitude of these side-band frequencies depend on the physical characteristics the rotor.

For example, the first left side-band frequency generated by the 400 Hz carrier ($n_s = 1$), varies between 350 Hz for 3000 rpm and 399 Hz for 60 rpm. The speed estimation is then based on the design of accurate filtering circuits, able to isolate the side-band frequencies from the carrier frequency. The filtering and isolation of the side-band frequencies have to be realized with special circuits because at low speeds, the difference between the carrier and the side-band frequencies (which contains the speed information) can be as small as one Hertz. Besides, the amplitude of the side-bands are very low compared with the carrier. This situation makes almost impossible to separate the side-bands from the carrier, using simple filters. The method used in this work to separate these frequencies is based on the principle of frequency multiplication, which permits to isolate the difference between the carrier and the particular side-band, Δf , through the amplification of the amplitude modulation as shown in Fig. 2. This figure shows the carrier current signal

obtained from the motor, which is successively self-multiplied, to get the information of Δf in the envelope of the carrier. When the carrier is self-multiplied, its frequency is duplicated and the amplitude variations due to the presence of side-band frequencies is made visible. The figure shows three successive multiplications, which permit to see clearly how Δf is amplified. The rotor speed is obtained by multiplying Δf by a constant number whose value depends on the side-band that has been isolated.

III. CIRCUIT DESIGN FOR SPEED DETECTION

The voltage amplitude of the carrier signal has been set in 15% of the nominal value of the fundamental. In this form, parasitic torque are small enough and then they will not produce pulsation problems. As the amplitude of the carrier is only 15% the nominal voltage of the machine, the side-band frequencies are extremely small. As an example, the Fig. 3 shows the frequency spectrum of the stator current obtained when a four pole machine is fed with a fundamental of 55 Hz and rotates at 1640 rpm. The fundamental and the 400 Hz carrier with their respective first side-bands frequencies, according with eq.(1), can be observed. The side-band frequencies are ubicated simetrically with respect to the corresponding fundamental. The first step is then to increase the amplitude of the carrier with respect to the main frequency of the inverter.

To increase the amplitude of the carrier signal with respect to the fundamental, the signal is filtered and amplified with respect to the mains frequency current and then multiplied by itself. This multiplication allows the separation of the main frequencies from the side-band frequencies through the sum, difference and double frequencies which appear in this operation. After the multiplication of the signal, another filtering through a low-pass filter is required from where the frequency spectrum shown in Fig. 4 is obtained. In the process, the biggest amplitude (without considering the dc

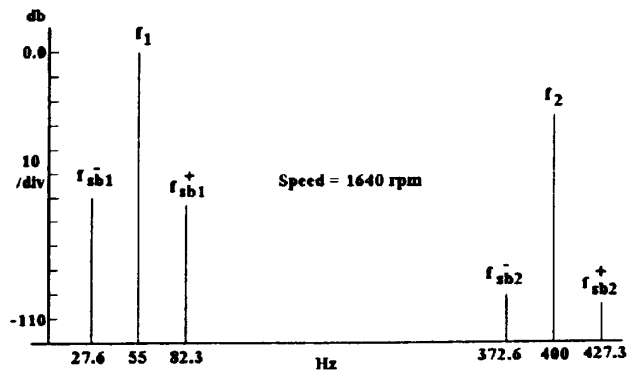


Fig. 3. Frequency spectrum of the stator signal.

component which is easily filtered) corresponds to a difference frequency, Δf , which is the basis of the speed evaluation. The large magnitude of Δf , A_{Δ} , is due to the addition of four amplitudes: $A[f_{sb1}^+ - f_1]$, $A[f_1 - f_{sb1}^-]$, $A[f_{sb2}^+ - f_2]$ and $A[f_2 - f_{sb2}^-]$, which correspond to the difference between the fundamental with their first-side-bands and the carrier with their side bands respectively. The high magnitude reached by Δf allows the computation of the rotor speed. The switching frequency of the inverter, which has neither been mentioned nor been taking in account, also contributes to increase the value of Δf and for this reason it is not required to filter it. After all these computations, the mechanical speed can be evaluated from:

$$\omega_m = k \Delta f \quad [rpm] \quad (3)$$

where k is a constant whose value depends on the side-band frequency being isolated. For example, $k=60$ gives the value in rpm for a four pole machine, when the first side-band frequency has been computed. The value of Δf is evaluated through:

$$\Delta f = f_{sb1}^+ - f_1 = f_1 - f_{sb1}^- \quad [Hz] \quad (4)$$

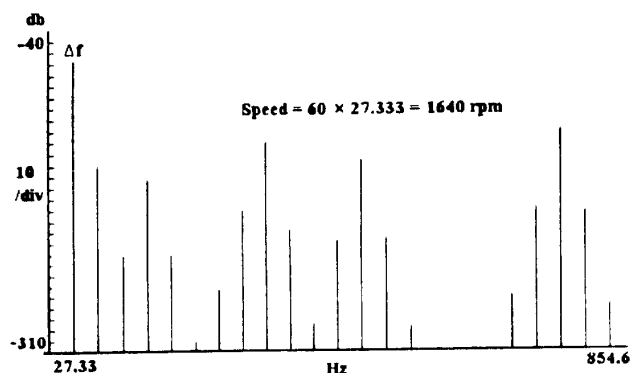


Fig. 4. Frequency spectrum after multiplication and filtering. (the highest amplitude corresponds to Δf)

The Fig. 5 shows the waveform generated with the spectrum of fig. 4. It can be noted that, despite the large amount of frequencies contained in this waveform, it looks almost sinusoidal, being Δf its main frequency, due to its high relative magnitude. Then the speed can be computed directly from the waveform of Fig. 4, with the help of an electronic counter.

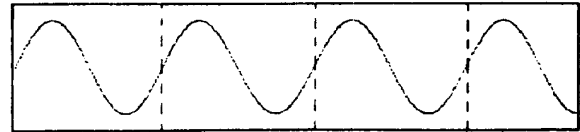


Fig. 5. Waveform generated with the spectrum of fig. 4

The Fig. 6 shows a functional block diagram of the overall system described, which comprises a high-pass filter to increase the magnitude of the carrier with respect to the main inverter frequency and then a couple of multipliers connected in cascade. From the second multiplier, the envelope, which corresponds to Δf , is isolated through a low-pass filter and then compared with a dc signal to get a square waveform of Δf , which is proportional to the machine speed. In the very low speed region a high order frequency side-band is isolated to get speeds as low as 20 rpm.

IV. SIMULATIONS AND EXPERIMENTS

In the simulations it has been found that the method based on the detection of side-band frequencies can measure lower speeds than expected, due to a good separation between Δf and the others frequencies, as shown in Fig. 7. In this figure, the frequency spectrum which correspond to the first-side-band, for a speed of 50 rpm is displayed. However, the utilization of the first-side-band at these speeds, becomes unpractical, because the electronic counter has to wait at least half turn of the rotor to determine Δf . If a higher order side-band is used, which is possible with the 400 Hz carrier, smaller speeds in a shorter time can be measured.

Some experiments have been carried out using four different induction machines: i) a 2 HP, 4 pole, 220 volts, 50 Hz, ii) a 2 HP, 4 pole, 380 volts, 50 Hz, iii) a 5 HP, 4 pole, 380 volts, 50 Hz and iv) a 12 HP, 6 pole, 380 volts, 50 Hz. From all of them, the speed estimation using the proposed method was successful. The following figures shows the experimental results obtained with the first aforementioned machine.

The Fig. 8.a) shows the current waveform of the frequency carrier and Fig. 8.b) shows the output signal obtained after the carrier is multiplied by itself. The envelope which contains the information of Δf has been marked with circles in 8.b), allowing to see almost one period of this frequency.

The signal obtained from Fig. 8.b) is multiplied again and then filtered to get the envelope (Δf), which is shown in Fig.9. The frequency of this envelope corresponds to 250 rpm and $k=15$ (see eq.(3)).

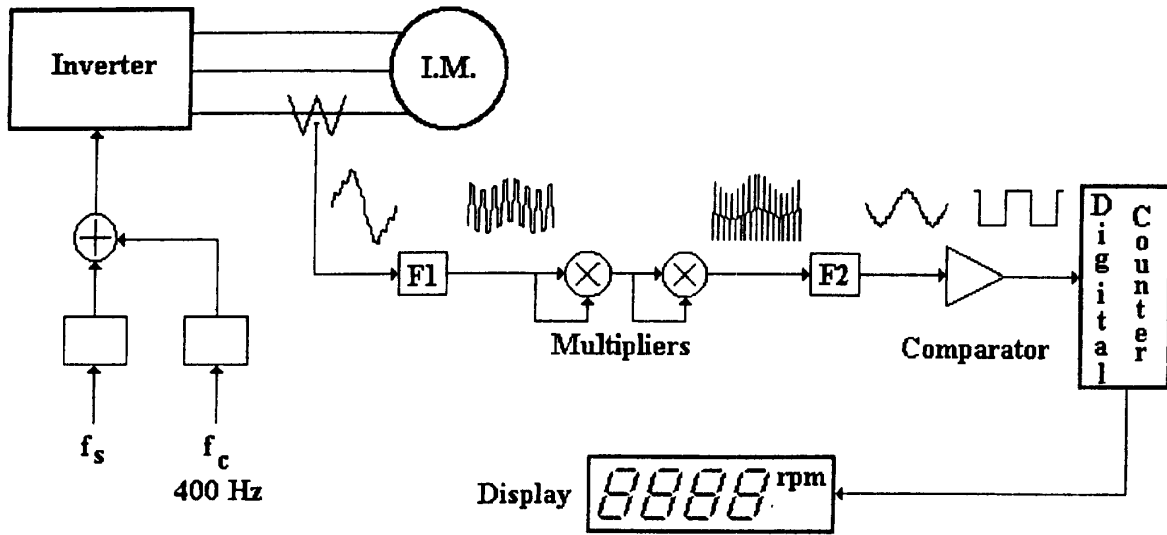


Fig. 6. Block diagram of the speed estimator circuit.

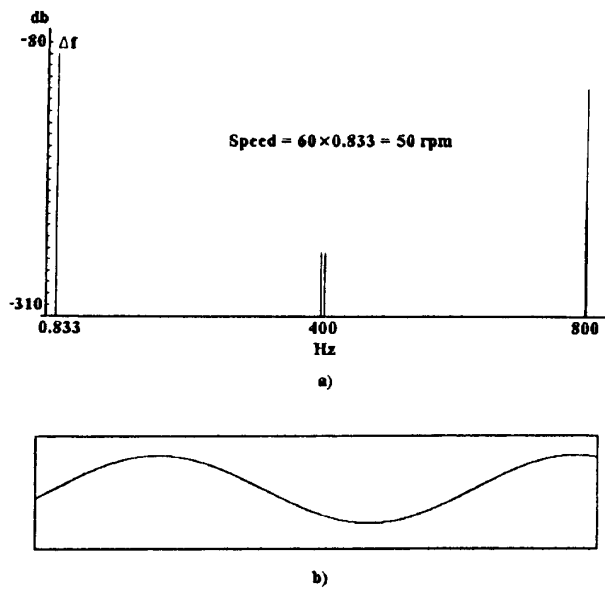


Fig. 7. Simulation results for a speed of 50 rpm
 a) frequency spectrum showing Δf
 b) waveform obtained from a)

This envelope is then compared with a constant signal to get a square waveform which is proportional to the speed machine. The Fig. 10 shows now the envelope Δf with its square waveform, for a speed of 565 rpm. Finally, the Fig. 11 shows Δf and its associated square waveform for a speed of 19 rpm. At this speed the waveforms are not so clear but the speed is still recognized. In this figure is also possible to see another frequency superimposed over Δf , which corresponds to a frequency generated by rotor slots. With a good filtering system, this new frequency could allow to measure even lower speeds.

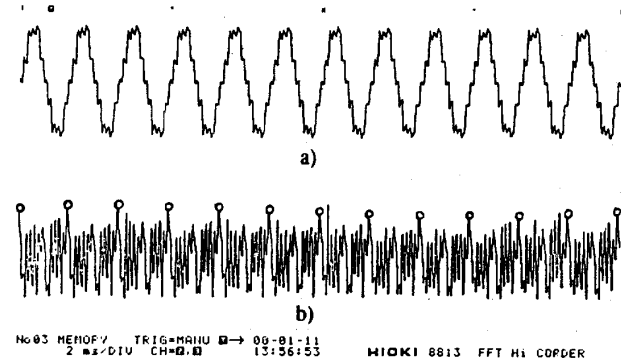


Fig. 8. a) frequency carrier waveform
 b) self-multiplication of the carrier

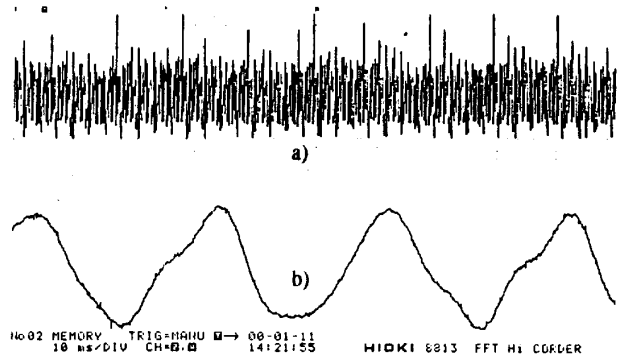


Fig. 9. a) self-multiplication of the carrier
 b) frequency envelope for 250 rpm

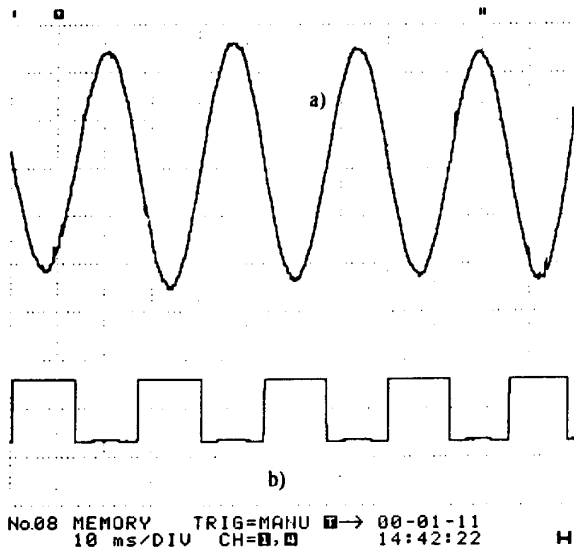


Fig. 10. Speed signals for 565 rpm
a) frequency envelope (Δf)
b) associated square waveform

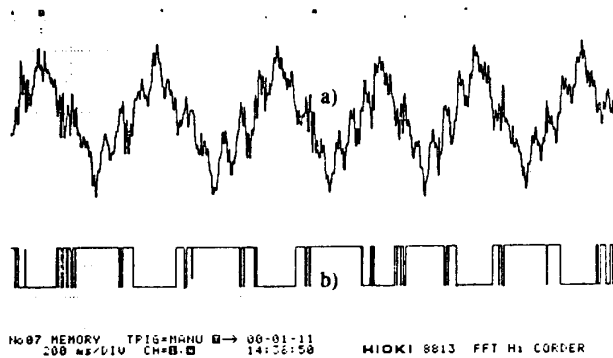


Fig. 11. Speed signals for 19 rpm
a) frequency envelope (Δf)
b) associated square waveform

It can also be mentioned that with the 12 HP, 6 poles machine tested, a speed of 2 rpm was computed with the circuit. This was possible because the harmonics generated by the rotor slots were large enough in amplitude to be measured and they produced 40 periods of Δf with just one turn of the rotor.

V. CONCLUSIONS

A different method to estimate the speed of induction motors is proposed. The method is based on the addition of a fixed carrier frequency signal to the PWM modulation. This carrier permits the detection of side-band frequencies generated by rotor eccentricities, which are subtracted from the carrier to obtain Δf . Depending on the order of the side-band which has been computed, Δf is multiplied by a constant to get the speed of the machine in rpm. The speed detection is independent of the electromagnetic parameters because the induced harmonics are based on the mechanical eccentricities of the rotor. It has also been verified that with some kind of induction motors, high order side-band

harmonics, produced by rotor slots, can be detected, making it possible to measure speeds as low as 2 rpm. However, with the motors tested in laboratory this was feasible in only one machine. Despite it, 20 rpm as a lowest speed limit for the other machines was possible by isolating the fourth-order side-band frequency.

Computer simulations and experiments with different induction machines have permitted to verify the feasibility of practical implementation.

ACKNOWLEDGMENTS

The authors want to thank Conicyt for the financial support to this work, through the Proyecto Fondecyt 652-93.

REFERENCES

- [1] A. Nabae and R. Kurosawa, "A New Induction Motor Drive System Having Constant Torque Transfer Function," *Trans. IEE Japan*, vol. 98B, Mar. 1978, pp.303-309.
- [2] W. Schumacher and W. Leonhard, "Transistor-Fed AC Servo Drive with Microprocessor Control," in *Conf. Rec. 1983 IPEC-Tokyo, Japan*, pp. 1465-1476.
- [3] T.A. Lipo and E.P. Cornell, "Modeling and Design of Controlled Current Induction Motor Drive System," *IEEE Trans. Ind. Appl.*, vol. IA-13, July/Aug. 1977, pp. 321-330.
- [4] A.B. Plunkett, "Direct Flux and Torque Regulation in a PWM Inverter-Induction Motor Drive," *IEEE Trans. Ind. Appl.*, vol. IA-13, Mar./Apr. 1977, pp. 139-146.
- [5] J. Pontt, J. Rodriguez and P. Pavez, "Control Analógico de un Motor de Inducción con Inversor PWM sin empleo de Tacómetro", *Anales VIII Congreso Chileno de Ingeniería Eléctrica*, 1989, pp. 14-18.
- [6] T.C. Green, B.W. Williams and D.S. Schramm, "Non-Invasive Speed Measurement of Inverter Driven Induction Motors," *IEEE Industry Applications Society, Annual meeting 1990*, pp. 395-398.
- [7] M. Ishida and K. Iwata, "A New Slip Frequency Detector and an Induction Motor Utilizing Rotor Slot Harmonics," *IEEE trans. Ind. Appl.*, vol. IA-20, May/June 1984, pp. 575-582.
- [8] M. Ishida and K. Iwata, "Steady-State Characteristics of a Torque and Speed Control System of an Induction Motor Utilizing Rotor Slot Harmonics for Slip Frequency Sensing," *IEEE Trans. Power Elect.*, vol. PE-2, N°3, July 1987, pp. 257-260.